

Transferring multiqubit entanglement onto memory qubits in a decoherence-free subspace

Xiao-Ling He¹ and Chui-Ping Yang^{2*}

¹*School of Science, Zhejiang University of Science and Technology, Hangzhou, Zhejiang 310023, China*

²*Department of Physics, Hangzhou Normal University, Hangzhou, Zhejiang 310036, China and*

* *yangcp@hznu.edu.cn*
(Dated: March 4, 2022)

Different from the previous works on generating entangled states, this work is focused on how to transfer the prepared entangled states onto memory qubits for protecting them against decoherence. We here consider a physical system consisting of n operation qubits and $2n$ memory qubits placed in a cavity or coupled to a resonator. A method is presented for transferring n -qubit Greenberger-Horne-Zeilinger (GHZ) entangled states from the operation qubits (i.e., information processing cells) onto the memory qubits (i.e., information memory elements with long decoherence time). The transferred GHZ states are encoded in a decoherence-free subspace against collective dephasing, and thus can be immune from decoherence induced by a dephasing environment. In addition, the state transfer procedure has nothing to do with the number of qubits, the operation time does not increase with the number of qubits, and no measurement is needed for the state transfer. This proposal can be applied to a wide range of hybrid qubits such as natural atoms and artificial atoms (e.g., various solid-state qubits).

PACS numbers: 03.67.Bg, 42.50.Dv, 85.25.Cp, 76.30.Mi

I. INTRODUCTION

Greenberger-Horne-Zeilinger (GHZ) states are of great interest in the fundamental test of quantum mechanics [1] and may prove to be useful in quantum metrology [2] and high-precision spectroscopy [3-5]. They have many applications in quantum information processing (QIP) and quantum communication such as quantum teleportation [6,7], entanglement swapping [8], quantum cryptographic [9], and error correction protocols [10,11]. During the past decade, a great deal of efforts has been devoted to generating GHZ states in various physical systems. For example, based on cavity or circuit QED, many theoretical methods have been presented for generating multiqubit GHZ states with atoms [12], quantum dots [13,14], and superconducting qubits [15-18]. A natural question on how to store the prepared GHZ states and how to protect them against decoherence would become interesting and important.

Hybrid quantum systems, composed of different kinds of qubits, have attracted tremendous attentions recently [19-27]. In addition, cavity or circuit QED has been considered as one of the most promising candidates for implementing large-scale QIP [28-30]. When two sets of qubits placed in a cavity or resonator are hybrid (i.e., different types), qubits in one set can act as information processing cells (i.e., the operation qubits) while qubits in the other set play a role of information memory elements (i.e., the memory qubits). Here, the operation qubits are readily controlled and thus used for performing quantum operations, while the memory qubits have long decoherence time and thus are good to be used for storing quantum states. It is well known that multiqubit entangled states are essential resources for large-scale QIP. When performing QIP in a hybrid system, after a step of information processing is completed, one needs to transfer entangled states of operation qubits to memory qubits for storage; and one needs to transfer the entangled states from the memory qubits back to the operation qubits when a further step of processing is needed.

It has been recognized that decoherence resulting from the coupling of the system with environment is one of the main obstacles in realizing a quantum information processor. Generally speaking, the effect of decoherence in carrying out QIP can be minimized as long as the typical operation time for performing various quantum operations is much shorter than the decoherence time of the system involved in QIP. In contrast, decoherence may pose a significant issue during the storage of quantum states (especially in the case when quantum states are stored for a long time). Hence, how to protect quantum states from decoherence is important in achieving an efficient storage of quantum states.

Motivated by the above, in this work we focus on how to transfer multiqubit entangled states from operation qubits onto memory qubits, and how to protect the transferred multiqubit entangled states against decoherence induced due to interacting with phase-dumping environments during the storage. Note that phase dumping can be a dominating decoherence source for noise environments, which has been widely studied over the past years [31-38].

In the following, we consider a physical system which consists of n operation qubits and $2n$ memory qubits placed in a cavity or coupled to a resonator. We will propose a method to transfer an n -qubit GHZ state $\alpha|00\dots0\rangle + \beta|11\dots1\rangle$

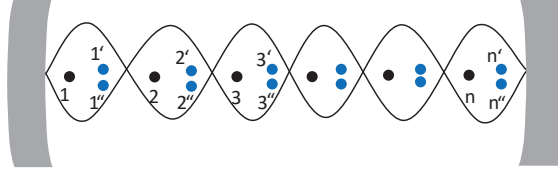


FIG. 1: (Color online) Diagram of operation qubits and memory qubits in a cavity or a resonator. The two dashed curves represent the standing-wave cavity mode. Each dark dot or blue dot represents a qubit. The dark dots represent operation qubits $(1, 2, \dots, n)$ while the blue dots denote the memory qubits $(1', 2', \dots, n', 1'', 2'', \dots, n'')$. Qubits $\{1', 1''\}$, qubits $\{2', 2''\}$, ..., or qubits $\{n', n''\}$ are arranged to be close (compared to the environment's coherence length), such that the two memory qubits in each pair couple to the environment in the same way appropriately.

(with arbitrary coefficients α and β) from n operation qubits onto $2n$ memory qubits, in the form of $\alpha|0101\dots01\rangle + \beta|1010\dots10\rangle$ encoded in a decoherence-free subspace (DFS) against collective dephasing. The DFS here is spanned by the basis vectors $|01\rangle$ and $|10\rangle$ of every two memory qubits. As shown below, this approach has the following advantages: (i) Since the transferred GHZ states are encoded within a DFS, they are immune from dephasing during the storage on the memory qubits; (ii) This protocol can be used to transfer the GHZ states deterministically; (iii) The state transfer procedure needs only a few basic operations, which does not depend on the number of qubits; (iv) The operation time does not increase as the number of qubits increases; (v) no measurement is needed; (vi) During the operation, the level $|f\rangle$ only for two qubits is occupied and thus decoherence from the qubits is greatly suppressed. This proposal can be applied to implement the GHZ state transfer between various hybrid qubits such as natural atoms and artificial atoms [e.g., quantum dots, nitrogen-vacancy (NV) centers, superconducting qubits, etc.]. To the best of our knowledge, how to transfer entangled states onto memory qubits in a DFS, based on cavity/circuit QED, has not been investigated until today.

This paper is organized as follows. In Sect. II, we show a general method to transfer GHZ entangled states from n operation qubits to $2n$ memory qubits encoded in a DFS against collective dephasing. In Sect. III, we give a brief discussion on the experimental issues, we then discuss the experimental feasibility of transferring a three-qubit GHZ state from superconducting flux qubits to superconducting transmon qubits in a DFS based on circuit QED. A concluding summary is presented in Sect. IV.

II. TRANSFERRING GHZ STATES ONTO MEMORY QUBITS IN A DFS

Consider two sets of hybrid qubits in a cavity or resonator (Fig. 1). The first set contains n identical operation qubits $(1, 2, \dots, n)$, the second set contains $2n$ identical memory qubits $(1', 2', \dots, n', 1'', 2'', \dots, n'')$, but qubits in different sets are non-identical or hybrid. Each qubit here is associated with a three-level quantum system (Fig. 2), with the two levels $|g\rangle$ and $|e\rangle$ representing a qubit and the third level $|f\rangle$ used for the state manipulation. Before the GHZ state transfer, the level structure of qubit 1 is adjusted to be different from that of qubits $(2, 3, \dots, n)$, and the level structure of qubit $1'$ is adjusted to be different from that of qubits $(2', 3', \dots, n', 1'', 2'', \dots, n'')$ (Fig. 2). Note that the level spacings of superconducting qubits can be rapidly (within a few nanoseconds [39-41]) adjusted by varying external control parameters (e.g., the magnetic flux applied to the superconducting loop of qubits; see e.g. [28,39,42,43]), the level spacings of NV centers can be adjusted by changing the external magnetic field applied to the NV centers [44,45], and the level spacings of atoms or quantum dots can be adjusted by changing the voltage on the electrodes around each atom/quantum dot [46].

Each qubit is initially decoupled from the cavity (Fig. 2). Suppose that the n operation qubits $(1, 2, \dots, n)$ are initially in a GHZ state

$$|\text{GHZ}\rangle_{12\dots n} = \alpha \prod_{l=1}^n |g\rangle_l + \beta \prod_{l=1}^n |e\rangle_l \quad (1)$$

(with normalized unknown factors α and β).

Note that the state $|\text{GHZ}\rangle_{12\dots n}$ of the n operation qubits $(1, 2, \dots, n)$ can be prepared using the existing schemes (e.g., [12-18]). By applying classical pulses to the operation qubit 1, the states $|g\rangle_1$ and $|e\rangle_1$ can be easily converted into the states $|e\rangle_1$ and $|f\rangle_1$, respectively. Also, by applying classical pulses to the operation qubits $(2, 3, \dots, n)$, one

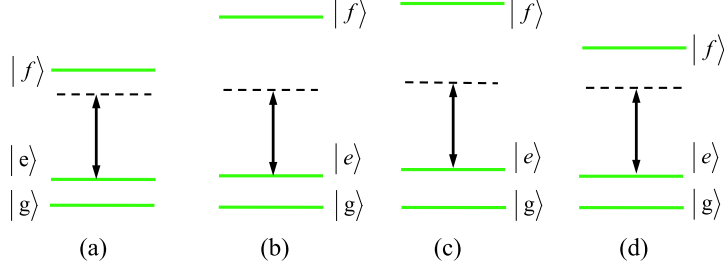


FIG. 2: (Color online) Level structure of each qubit before the GHZ state transfer. (a), (b), (c), and (d) represent the level structures for qubit 1, qubits (2, 3, ..., n), qubits (2', 3', ..., n', 1'', 2'', ..., n''), and qubit 1', respectively. Each double-arrow vertical line represents the cavity frequency (not adjusted), which is highly detuned from the transition frequency between any two levels of each qubit. Thus, each qubit is initially decoupled from the cavity before the GHZ state transfer. The difference between the level structures of (a) and (b) [(c) and (d)] can be readily achieved by adjusting the level spacings of qubit 1 (qubit 1') before the GHZ state transfer [28,39,42-46]. For simplicity, here and in Fig. 3, we consider the case that the spacing between the levels $|g\rangle$ and $|e\rangle$ is smaller than that between the levels $|e\rangle$ and $|f\rangle$. Alternatively, the spacing between the levels $|g\rangle$ and $|e\rangle$ can be larger than that between the levels $|e\rangle$ and $|f\rangle$.

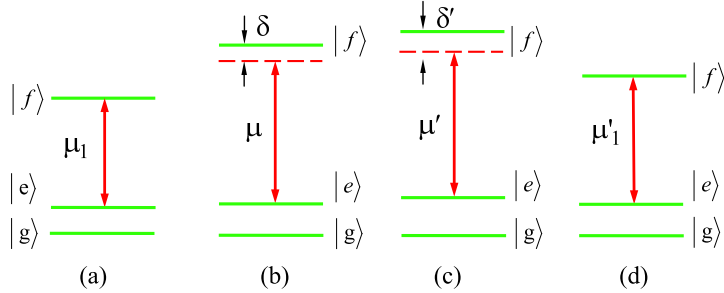


FIG. 3: (Color online) Illustration of qubit-cavity interaction. (a) The cavity resonantly interacts with the $|e\rangle \leftrightarrow |f\rangle$ transition of qubit 1. (b) The cavity dispersively interacts with the $|e\rangle \leftrightarrow |f\rangle$ transition of qubits (2, 3, ..., n). (c) The cavity dispersively interacts with the $|e\rangle \leftrightarrow |f\rangle$ transition of qubits (2', 3', ..., n', 1'', 2'', ..., n''). (d) The cavity resonantly interacts with the $|e\rangle \leftrightarrow |f\rangle$ transition of qubit 1'. The level $|g\rangle$ of each qubit is not affected by the cavity as long as the $|g\rangle \leftrightarrow |e\rangle$ and $|g\rangle \leftrightarrow |f\rangle$ transitions are forbidden or highly detuned (i.e., decoupled) from the cavity mode

can convert the states $|g\rangle$ and $|e\rangle$ of each of these operation qubits into the states $|+\rangle$ and $|-\rangle$, respectively. Here and below, $|\pm\rangle = (|g\rangle \pm |e\rangle)/\sqrt{2}$ are two orthogonal states. Thus, the GHZ state $|\text{GHZ}\rangle_{12\dots n}$ of the operation qubits can be written as

$$|\text{GHZ}\rangle_{12\dots n} = \alpha \prod_{l=2}^n |+\rangle_l |e\rangle_1 + \beta \prod_{l=2}^n |-\rangle_l |f\rangle_1. \quad (2)$$

Assume that the $2n$ memory qubits (1', 2', ..., n', 1'', 2'', ..., n'') are in the state $|e\rangle_{1'}, \prod_{l'=2'}^{n'} |+\rangle_{l'}, \prod_{l''=1''}^{n''} |-\rangle_{l''}$, which can be prepared by applying classical pulses to the memory qubits (1', 2', ..., n', 1'', 2'', ..., n'') each initially in the ground state $|g\rangle$. Suppose that the cavity is initially in a vacuum state $|0\rangle_c$. Thus, the initial state of the whole system is given by

$$\left(\alpha \prod_{l=2}^n |+\rangle_l |e\rangle_1 + \beta \prod_{l=2}^n |-\rangle_l |f\rangle_1 \right) |e\rangle_{1'} \prod_{l'=2'}^{n'} |+\rangle_{l'} \prod_{l''=1''}^{n''} |-\rangle_{l''} |0\rangle_c. \quad (3)$$

For simplicity, in the following we will use the phrase “ $|e\rangle \leftrightarrow |f\rangle$ transition” to represent the “transition between the levels $|e\rangle$ and $|f\rangle$ ”. Similar phrases are used to represent the transition between the levels $|g\rangle$ and $|e\rangle$ as well as the transition between the levels $|g\rangle$ and $|f\rangle$.

From the description given below, one can see that there is no need of adjusting the qubit level spacings during the entire GHZ state transfer. The whole procedure for transferring the GHZ state $|\text{GHZ}\rangle_{12\dots n}$ of the n operation qubits $(1, 2, \dots, n)$ onto the $2n$ memory qubits $(1', 2', \dots, n', 1'', 2'', \dots, n'')$ is listed as follows:

Step (i): Bring the cavity resonant with the $|e\rangle \leftrightarrow |f\rangle$ transition of qubit 1 [Fig. 3(a)]. The Hamiltonian describing this operation is given by $H_I = \hbar(\mu_1 a^+ |e\rangle_1 \langle f|) + h.c.$, where a^+ is the photon creation operator of the cavity mode, and μ_1 is the resonant coupling constant between the cavity and the $|e\rangle \leftrightarrow |f\rangle$ transition of qubit 1. Under the Hamiltonian H_I , the state component $|e\rangle_1 |0\rangle_c$ is not changed because of $H_I |e\rangle_1 |0\rangle_c = 0$. However, after an interaction time $t_1 = \pi/(2\mu_1)$ (i.e., half a Rabi oscillation), the state $|f\rangle_1 |0\rangle_c$ changes to $-i|e\rangle_1 |1\rangle_c$ (for the details, see [47]). Hence, the initial state (1) of the whole system becomes

$$\left(\alpha \prod_{l=2}^n |+\rangle_l |0\rangle_c - i\beta \prod_{l=2}^n |-\rangle_l |1\rangle_c \right) |e\rangle_1 |e\rangle_{1'} \prod_{l'=2'}^{n'} |+\rangle_{l'} \prod_{l''=1''}^{n''} |-\rangle_{l''}. \quad (4)$$

Step (ii): Bring the cavity dispersively coupled with the $|e\rangle \leftrightarrow |f\rangle$ transition of operation qubits $(2, 3, \dots, n)$, with non-resonant coupling strength μ and detuning $\delta = \omega_{fe} - \omega_c$ [Fig. 3(b)]. Meanwhile, the cavity is dispersively coupled to the $|e\rangle \leftrightarrow |f\rangle$ transition of memory qubits $(2', 3', \dots, n', 1'', 2'', \dots, n'')$, with non-resonant coupling strength μ' and detuning $\delta' = \omega'_{fe} - \omega_c$ [Fig. 3(c)]. Here, ω_{fe} (ω'_{fe}) is the transition frequency between the levels $|e\rangle$ and $|f\rangle$ for operation qubits $(2, 3, \dots, n)$ [memory qubits $(2', 3', \dots, n', 1'', 2'', \dots, n'')$], ω_c is the (adjusted) cavity frequency. In the interaction picture, the Hamiltonian is given by (setting $\hbar = 1$)

$$\begin{aligned} H = & \mu \sum_{l=2}^n (e^{-i\delta t} |e\rangle_l \langle f| a^+ + h.c.) + \mu' \sum_{l'=2'}^{n'} (e^{-i\delta' t} |e\rangle_{l'} \langle f| a^+ + h.c.) \\ & + \mu' \sum_{l''=1''}^{n''} (e^{-i\delta' t} |e\rangle_{l''} \langle f| a^+ + h.c.). \end{aligned} \quad (5)$$

Under the large detuning conditions $\delta \gg \mu$ and $\delta' \gg \mu'$, there is no energy exchange between the qubits and the cavity mode. Then, the system dynamics described by the Hamiltonian of Eq. (5) is equivalent to that determined

by the following effective Hamiltonian [48-50]

$$\begin{aligned}
H = & \lambda \sum_{l=2}^n (|f\rangle_l \langle f| aa^+ - |e\rangle_l \langle e| a^+ a) \\
& + \lambda' \sum_{l'=2'}^{n'} (|f\rangle_{l'} \langle f| aa^+ - |e\rangle_{l'} \langle e| a^+ a) \\
& + \lambda' \sum_{l''=1''}^{n''} (|f\rangle_{l''} \langle f| aa^+ - |e\rangle_{l''} \langle e| a^+ a) \\
& + \lambda \sum_{l,k=2}^n |f\rangle_l \langle e| \otimes |e\rangle_k \langle f| \\
& + \lambda' \sum_{l',k'=2'}^{n'} |f\rangle_{l'} \langle e| \otimes |e\rangle_{k'} \langle f| \\
& + \lambda' \sum_{l'',k''=1''}^{n''} |f\rangle_{l''} \langle e| \otimes |e\rangle_{k''} \langle f| \\
& + \tilde{\lambda} \sum_{l=2,k'=2'}^{n,n'} e^{i(\delta-\delta')t} |f\rangle_l \langle e| \otimes |e\rangle_{k'} \langle f| \\
& + \tilde{\lambda} \sum_{l=2,k''=1''}^{n,n''} e^{i(\delta-\delta')t} |f\rangle_l \langle e| \otimes |e\rangle_{k''} \langle f| \\
& + \lambda' \sum_{l'=2',k''=1''}^{n',n''} |f\rangle_{l'} \langle e| \otimes |e\rangle_{k''} \langle f|, \tag{6}
\end{aligned}$$

where $\lambda = \mu^2/\delta$, $\lambda' = (\mu')^2/\delta'$, $\tilde{\lambda} = \frac{\delta\delta'}{2}(\frac{1}{\delta} + \frac{1}{\delta'})$, $l \neq k$ (line 4), $l' \neq k'$ (line 5), and $l'' \neq k''$ (line 6). The terms in lines 1, 2, and 3 of Eq. (6) describe the photon-number dependent Stark shifts. The term in line 4 describes the “dipole” couplings between the l th operation qubit and the k th operation qubit. The term in line 5 represents the “dipole” couplings between the l' th memory qubit and the k' th memory qubit. The term in line 6 denotes the “dipole” couplings between the l'' th memory qubit and the k'' th memory qubit. The terms in the last three lines describe the “dipole” coupling between the l th operation qubit and the k' th memory qubit, the l th operation qubit and the k'' th memory qubit, as well as the l' th memory qubit and the k'' th memory qubit, mediated by the cavity. Note that the level $|f\rangle$ of each qubit is not involved in Eq. (4). Thus, one can easily find that only the terms $-\lambda \sum_{l=2}^n |e\rangle_l \langle e| a^+ a$, $-\lambda' \sum_{l'=2'}^{n'} |e\rangle_{l'} \langle e| a^+ a$, and $-\lambda' \sum_{l''=1''}^{n''} |e\rangle_{l''} \langle e| a^+ a$ of Eq. (6) have contribution to the time evolution of the state (4), while all other terms in Eq. (6) acting on the state (4) result in zero. In other words, with respect to the state (4), the Hamiltonian (6) reduces to

$$H = -\lambda \sum_{l=2}^n |e\rangle_l \langle e| a^+ a - \lambda' \sum_{l'=2'}^{n'} |e\rangle_{l'} \langle e| a^+ a - \lambda' \sum_{l''=1''}^{n''} |e\rangle_{l''} \langle e| a^+ a. \tag{7}$$

Under the Hamiltonian (7), the state (4) evolves into

$$\begin{aligned}
& \left[\alpha \prod_{l=2}^n |+\rangle_l \prod_{l'=2'}^{n'} |+\rangle_{l'} \prod_{l''=1''}^{n''} |-\rangle_{l''} |0\rangle_c - i\beta \prod_{l=2}^n (|g\rangle_l - e^{i\lambda t} |e\rangle_l) \right. \\
& \left. \times \prod_{l'=2'}^{n'} (|g\rangle_{l'} + e^{i\lambda' t} |e\rangle_{l'}) \prod_{l''=1''}^{n''} (|g\rangle_{l''} - e^{i\lambda' t} |e\rangle_{l''}) |1\rangle_c \right] |e\rangle_1 |e\rangle_{1'} \tag{8}
\end{aligned}$$

In the case of $t_2 = (2m + 1)\pi/\lambda = (2k + 1)\pi/\lambda'$ (m and k are zero or positive integers), we have from Eq. (8)

$$\left[\alpha \prod_{l'=2'}^{n'} |+\rangle_{l'} \prod_{l''=1''}^{n''} |-\rangle_{l''} |0\rangle_c - i\beta \prod_{l'=2'}^{n'} |-\rangle_{l'} \prod_{l''=1''}^{n''} |+\rangle_{l''} |1\rangle_c \right] \prod_{l=2}^n |+\rangle_l |e\rangle_1 |e\rangle_{1'}. \quad (9)$$

Step (iii): Bring the cavity resonant with the $|e\rangle \leftrightarrow |f\rangle$ transition of qubit $1'$ [Fig. 3(d)]. The Hamiltonian describing this operation is given by $H_I = \hbar(\mu_{1'} a^\dagger |e\rangle_{1'} \langle f|) + h.c.$, where $\mu_{1'}$ is the resonant coupling constant between the resonator and the $|e\rangle \leftrightarrow |f\rangle$ transition of qubit $1'$. After an interaction time $t_3 = 3\pi/(2\mu_{1'})$, the resonator mode and qubit $1'$ undergo the transformation $|e\rangle_{1'} |0\rangle_c \rightarrow |e\rangle_{1'} |0\rangle_c$ and $|e\rangle_{1'} |1\rangle_c \rightarrow i|f\rangle_{1'} |0\rangle_c$. Thus, the state (9) becomes

$$\left[\alpha \prod_{l'=2'}^{n'} |+\rangle_{l'} \prod_{l''=1''}^{n''} |-\rangle_{l''} |e\rangle_{1'} + \beta \prod_{l'=2'}^{n'} |-\rangle_{l'} \prod_{l''=1''}^{n''} |+\rangle_{l''} |f\rangle_{1'} \right] \prod_{l=2}^n |+\rangle_l |e\rangle_1 |0\rangle_c. \quad (10)$$

By comparing Eq. (10) with Eq. (3) or Eqs. (1-2), one can see that the original n -qubit GHZ state of qubits $(1, 2, \dots, n)$ has been transferred onto the memory qubits $(1', 2', \dots, n', 1'', 2'', \dots, n'')$ after the operation. After this step of operation, the cavity frequency needs to be adjusted back to its original frequency (Fig. 2) such that the qubit system is decoupled from the cavity.

Note that by applying classical pulses to the qubit $1'$, the states $|e\rangle_{1'}$ and $|f\rangle_{1'}$ can be easily converted into the states $|g\rangle_{1'}$ and $|e\rangle_{1'}$, respectively. Also, by applying classical pulses to the memory qubits $(2', \dots, n', 1'', 2'', \dots, n'')$, one can convert the states $|+\rangle$ and $|-\rangle$ of each of the memory qubits $(2', \dots, n', 1'', 2'', \dots, n'')$ into the states $|g\rangle$ and $|e\rangle$, respectively. In this case, the entangled GHZ state of the $2n$ memory qubits, i.e., the left part in the square bracket of Eq. (10), will become

$$\begin{aligned} |\text{GHZ}\rangle_{DF} &= \alpha \prod_{l'=1'}^{n'} |g\rangle_{l'} \prod_{l''=1''}^{n''} |e\rangle_{l''} + \beta \prod_{l'=1'}^{n'} |e\rangle_{l'} \prod_{l''=1''}^{n''} |g\rangle_{l''} \\ &= \alpha |ge\rangle_{1'1''} |ge\rangle_{2'2''} \dots |ge\rangle_{n'n''} + \beta |eg\rangle_{1'1''} |eg\rangle_{2'2''} \dots |eg\rangle_{n'n''}. \end{aligned} \quad (11)$$

The state (11) is exactly a GHZ entangled state encoded within a DFS against collective dephasing, which is spanned by the basis vectors $|ge\rangle$ and $|eg\rangle$ of every two of paired memory qubits $\{1', 1''\}, \{2', 2''\}, \dots, \{n', n''\}$. When the two memory qubits in each pair undergo a collective decoherence, this encoded GHZ state (11) is immune to a phase-dumping environment because of $H|\text{GHZ}\rangle_{DF} = 0$, where $H = \sum_{j=1}^n g_j E \otimes (\sigma_{j',z} + \sigma_{j'',z})$ is an interaction Hamiltonian describing the $2n$ memory qubits interacting with a dephasing environment [31-33,37]. Here, E is an arbitrary environment operator, g_j is the coupling constant of the two paired memory qubits (j', j'') with the noise environment, $\sigma_{j',z} = |e\rangle_{j'} \langle e| - |g\rangle_{j'} \langle g|$ and $\sigma_{j'',z} = |e\rangle_{j''} \langle e| - |g\rangle_{j''} \langle g|$ are the operators of qubits j' and j'' respectively. By comparing Eq.(1) with Eq.(11), one can see that only two memory qubits are needed to protect one of GHZ qubits against decoherence caused by the dephasing environment.

Tuning the cavity frequency has been reported in various experiments for both optical cavities and microwave cavities [51-54]. For instance, the rapid tuning of cavity frequencies in 1 – 3 nanoseconds has been experimentally demonstrated for a superconducting transmission line resonator [53,54]. We should mention that adjusting the cavity frequency is unnecessary for this proposal. Alternatively, the qubit-cavity resonant interaction and the qubit-cavity dispersive interaction, which are required by the GHZ state transfer, can be achieved by adjusting the level spacings of the qubits [28,39,42-46].

Several points may need to be addressed here. First, the GHZ state transfer only employs the coupling of the cavity with the $|e\rangle \leftrightarrow |f\rangle$ transition of each qubit (Fig. 3). Hence, this proposal is applicable to qubits with forbidden $|g\rangle \leftrightarrow |e\rangle$ and $|g\rangle \leftrightarrow |f\rangle$ transitions. It also applies to qubits with $|g\rangle \leftrightarrow |e\rangle$ and $|g\rangle \leftrightarrow |f\rangle$ transitions as long as these transitions are highly detuned (i.e., decoupled) from the cavity, which can be achieved by adjusting the qubits' level spacings before performing the GHZ state transfer [28,39,42-46]. Second, as shown above, the level $|f\rangle$ for operation qubits $(2, 3, \dots, n)$ and memory qubits $(2', 3', \dots, n', 1'', 2'', \dots, n'')$ is unpopulated, i.e., the level $|f\rangle$ is occupied only for the two qubits 1 and $1'$ during the entire operation. Third, the operations for transferring GHZ states have nothing to do with α and β . Last, the method is applicable to a 1D, 2D or 3D cavity or resonator as long as the conditions described above can be met.

We should mention that since no measurement is involved during the GHZ state transfer, it is straightforward to show that the transferred GHZ state can be transferred back onto the operation qubits from the memory qubits by performing the inverse operations of the above unitary operations.

Note that the GHZ state given in Eq. (1) is an n -qubit quantum secret sharing code for encoding an arbitrary single-qubit pure state $\alpha|g\rangle + \beta|e\rangle$ [55], while the transferred GHZ state given in Eq. (11) is a quantum secret sharing

encoded with n pairs of memory qubits in a DFS. Thus, this proposal also provides a way to transfer quantum secret sharing from n operation qubits to n pairs of memory qubits in a DFS. The state in Eq. (11) may also be usable for keeping a resource of controlled quantum teleportation.

Note that a SWAP gate on qubits a and b , described by the state transformation $|i\rangle_a |j\rangle_b \rightarrow |j\rangle_a |i\rangle_b$ with $i, j \in \{0, 1\}$, can be used to implement the state transfer from qubit a to qubit b or vice versa. Thus, it is straightforward to show that the transfer of an n -qubit GHZ state, considered in this work, can be completed with n SWAP gates each acting on an operation qubit and a memory “logical qubit”. Here, a memory logical qubit consists of two memory qubits (e.g., qubit pair $1'1'', 2'2'', \dots$, or $n'n''$), whose two logical states are the states $|ge\rangle$ and $|eg\rangle$ which form a DFS against collective dephasing. According to [56], construction of a SWAP gate requires three CNOT gates, which can be realized by the idea presented in [57]. In this sense, $3n$ CNOT gates are needed for constructing n SWAP gates. Thus, at least $3n$ basic operations are necessary to transfer an n -qubit GHZ state from the n operation qubits to the $2n$ memory qubits, provided that a CNOT gate can be realized with one basic operation only. In stark contrast, as shown above, the present proposal requires only a few operational steps to transfer an n -qubit GHZ state, which is independent of n .

Based on cavity/circuit QED, there exist a number of schemes for generating the GHZ states in various types of qubits (e.g., Refs. [12-18]), which are based on qubit-cavity resonant interaction (QCRI) or dispersive interaction. As shown above, the GHZ state transfer is mainly based on step (ii), which was performed via the dispersive interaction. Regarding the operation speed, the GHZ state transfer is comparable to the GHZ state preparation based on dispersive interaction. This is because the GHZ state generation requires an initial state preparation of the qubit system.

When the number of qubits is large, the operational speed for the GHZ state transfer here may also be comparable to that of the GHZ state generation based on QCRI. Reasons for that are the following. The GHZ state preparation via QCRI requires a cavity photon resonantly interacting with each qubit sequentially, and thus step-by-step control is needed. Although each step can be performed fast due to using QCRI, the total operation time increases linearly with the number of qubits and becomes long when the number of qubits is large. However, as shown above, the procedure for the GHZ state transfer only needs a few operational steps and the operation time is independent of the number of qubits.

This work is also of interest from the following point of view. As mentioned in the introduction, we considered two sets of qubits, i.e., operation qubits and memory qubits. The operation qubits are readily controlled and thus preferable to be used for performing various quantum operations required by quantum computing. Compared to the memory qubits, the operation qubits have shorter decoherence time. Thus, the prepared GHZ states with the operation qubits are easy to be destroyed due to decoherence. One would need to repeat preparing them once they are destroyed. However, this problem is mitigated by transferring the GHZ states from the operation qubits onto the memory qubits for a long time storage.

III. DISCUSSION

For the method to work, the following requirements need to be satisfied:

(i) The condition $(2m+1)\pi/\lambda = (2k+1)\pi/\lambda'$ needs to be met. Because of $\lambda = \mu^2/\delta$ and $\lambda' = (\mu')^2/\delta'$, this condition can be readily reached with an appropriate choice of δ (or δ') via adjusting the level spacings of qubits $(2, 3, \dots, n)$ [or qubits $(2', 3', \dots, n', 1'', 2'', \dots, n'')$] or the coupling constant μ (μ') by varying the qubit locations in the cavity.

(ii) The total operation time is

$$\tau = \frac{\pi}{2\mu_1} + \frac{3\pi}{2\mu_{1'}} + \frac{(2m+1)\pi}{\lambda} + \tau_p + 4\tau_d, \quad (12)$$

which is independent of the number of qubits. Here, t_d is the typical time required for adjusting the cavity frequency while τ_p is the typical time required for applying the classical pulses. The operation time τ should be much smaller than the energy relaxation time and the dephasing time of qubits. In addition, τ should be much smaller than the lifetime of the cavity mode, which is given by $\kappa^{-1} = Q/\omega_c$ (Q is the quality factor of the cavity). In principle, these requirements can be satisfied as follows. The operation time τ can be reduced by increasing the coupling constants μ and μ' , by shortening the pulse duration via increasing the pulse Rabi frequency, and by rapidly adjusting the cavity frequency (e.g., $\tau_d \sim 1 - 3$ ns is the typical time for adjusting the frequency of a microwave cavity in experiments [53,54]). In addition, κ^{-1} can be increased by employing a high- Q resonator. Note that the symbol “ \sim ” used here and below means “approximately equals to”.

(iii) During step (ii), the occupation probability p of the level $|f\rangle$ for each of operation qubits $(2, 3, \dots, n)$ and the

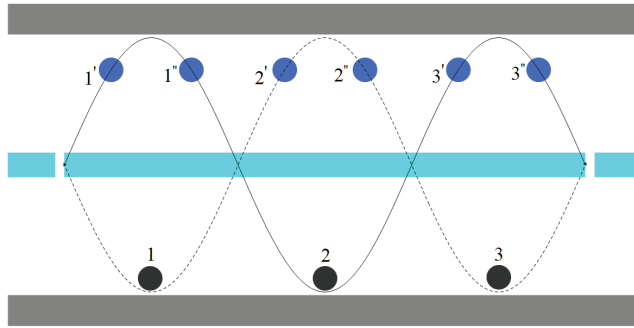


FIG. 4: (Color online) Setup for three superconducting flux qubits (black dots), six superconducting transmon qubits (blue dots), and a one-dimensional coplanar waveguide resonator. The two curved lines represent the standing wave magnetic field of the resonator. Here, the flux qubits (1, 2, 3) act as the operation qubits, while the paired transmon qubits, i.e., qubits $\{1', 1''\}$, qubits $\{2', 2''\}$, and qubits $\{3', 3''\}$, play a role of the memory qubits.

occupation probability p' of the level $|f\rangle$ for each of memory qubits ($2', 3', \dots, n', 1'', 2'', \dots, n''$) are given by [58]

$$p \simeq \frac{4\mu^2}{4\mu^2 + \delta^2},$$

$$p' \simeq \frac{4(\mu')^2}{4(\mu')^2 + (\delta')^2}. \quad (13)$$

The occupation probabilities p and p' need to be negligibly small in order to reduce the operation error. For the choice of $\delta = 10\mu$ and $\delta' = 10\mu'$, we have $p, p' \sim 0.04$, which can be further reduced by increasing the ratio of δ/μ and δ'/μ' .

For the sake of definitiveness, let us consider the experimental possibility of transferring a three-qubit GHZ state from three identical superconducting flux qubits to six identical superconducting transmon qubits embedded in a one-dimensional transmission line resonator (TLR) (Fig. 4). Flux qubits have stronger level anharmonicity (compared to transmon qubits) while transmon qubits have relatively long decoherence time reported in experiments. Thus, as an example, we here consider using flux qubits as operation qubits while transmon qubits as memory qubits. As a rough estimate, assume $\mu_1 \sim \mu \sim \mu' \sim \mu_{1'} \sim 2\pi \times 10$ MHz and $\delta \sim 10\mu$, $\delta' \sim 10\mu'$, resulting in $\lambda = \lambda'$ and thus $m = k = 0$ chosen for the shortest operation time τ . In addition, assume $\tau_d \sim 2$ ns, and $\tau_p \sim 10$ ns (readily available because a microwave pulse Rabi frequency $\Omega/2\pi \sim 300$ MHz has been reported in experiments [59]). Note that the coupling strengths with the values chosen here are readily available in experiments because a coupling strength ~ 636 MHz has been reported for a flux qubit coupled to a TLR [60] and a coupling constant ~ 220 MHz has been experimentally demonstrated for a transmon qubit coupled to a TLR [61]. For the parameters chosen here, we have $\tau \sim 0.6$ μ s, which is much shorter than the early-reported decoherence time 6 – 20 μ s of the flux qubits [62] and lifetime $\sim 50 - 80$ μ s for the transmon qubits [63,64]. For both flux qubits and transmon qubits, the typical transition frequency between two neighbor levels $|e\rangle$ and $|f\rangle$ can be made to be 5 – 10 GHz. Thus, as an example, choose $\omega_c \sim 5$ GHz. In addition, consider $Q \sim 5 \times 10^5$, and thus we have $\kappa^{-1} \sim 16$ μ s, which is much longer than the operation time $\tau \sim 0.6$ μ s given above. The required resonator quality factor here is achievable in experiment because TLRs with a (loaded) quality factor $Q \sim 10^6$ have been experimentally demonstrated [65,66]. The result presented here shows that transferring a three-qubit GHZ state from superconducting flux qubits onto superconducting transmon qubits in a DFS is possible within present-day circuit QED. We remark that further investigation is needed for each particular experimental setup. However, this requires a rather lengthy and complex analysis, which is beyond the scope of this theoretical work.

IV. CONCLUSION

We have shown that multi-qubit GHZ states can be deterministically transferred from the operation qubits onto the memory qubits, through only a few basic operations. Since the transferred GHZ states are encoded with memory qubits within a DFS, they are immune from dephasing environments, and thus can in principle be protected against decoherence caused by dephasing for an indefinite length of time (without the need for frequent checking). As shown above, the state transfer does not depend on the number of qubits, the operation time does not increase with the

number of qubits, and no measurement is needed during the entire operation. Moreover, since the level $|f\rangle$ only for two qubits was occupied during the operation, decoherence from the qubits is greatly suppressed. This proposal can be applied to a wide range of hybrid qubits such as natural atoms and artificial atoms (e.g., quantum dots, NV centers, and various superconducting qubits).

V. ACKNOWLEDGMENTS

This work was supported in part by the Ministry of Science and Technology of China under Grant No. 2016YFA0301802, the National Natural Science Foundation of China under Grant Nos. 11074062 and 11374083, and the Zhejiang Natural Science Foundation under Grant Nos. LZ13A040002 and LY15A040006. This work was also supported by the funds of Hangzhou City for supporting the Hangzhou-City Quantum Information and Quantum Optics Innovation Research Team.

-
- [1] Greenberger, D.M., Horne, M.A., Zeilinger, A.: Going beyond Bell theorem. In: Kafatos, M. (ed.) *Bell Theorem, Quantum Theory and Conceptions of the Universe*. Kluwer Academic, Dordrecht (1989)
 - [2] Giovannetti, V., Lloyd, S., Maccone, L.: Quantum-enhanced measurements: Beating the standard quantum limit. *Science* **306**, 1330 (2004)
 - [3] Bollinger, J.J., Itano, W.M., Wineland, D.J., Heinzen, D.J.: Optimal frequency measurements with maximally correlated states. *Phys. Rev. A* **54**, R4649 (1996)
 - [4] Bergquist, J.C., Jefferts, S.R., Wineland, D.J.: Time measurement at the millennium. *Phys. Today* **54**, 37 (2001)
 - [5] Leibfried, D., Barrett, M.D., Schaetz, T., Britton, J., Chiaverini, J., Itano, W.M., Jost, J.D., Langer, C., Wineland, D.J.: Toward Heisenberg-limited spectroscopy with multiparticle entangled states. *Science* **304**, 1476 (2004)
 - [6] Karlsson, A., Bourennane, M.: Quantum teleportation using three-particle entanglement. *Phys. Rev. A* **58**, 4394 (1998)
 - [7] Jung, E., Hwang, M.R., JuYou, H., Kim, M.S., Yoo, S.K., Kim, H., Park, D., Son, J.W., Tamaryan, S., Cha, S.K.: Greenberger-Horne-Zeilinger versus W states: quantum teleportation through noisy channels. *Phys. Rev. A* **78**, 012312 (2008)
 - [8] Lu, C.Y., Yang, T., Pan, J.W.: Experimental multiparticle entanglement swapping for quantum networking. *Phys. Rev. Lett.* **103**, 020501 (2009)
 - [9] Bennett, C.H., Wiesner, S.J.: Communication via one- and two-particle operators on Einstein-Podolsky-Rosen states. *Phys. Rev. Lett.* **69**, 2881 (1992)
 - [10] DiVincenzo, D.P., Shor, P.W.: Fault-tolerant error correction with efficient quantum codes. *Phys. Rev. Lett.* **77**, 3260 (1996)
 - [11] Preskill, J.: Reliable quantum computers. *Proc. R. Soc. Lond. Ser. A* **454**, 385 (1998)
 - [12] Zheng, S.B.: One-step synthesis of multiatom Greenberger-Horne-Zeilinger states. *Phys. Rev. Lett.* **87**, 230404 (2001)
 - [13] Wang, X., Feng, M., Sanders, B.C.: Multipartite entangled states in coupled quantum dots and cavity QED. *Phys. Rev. A* **67**, 022302 (2003)
 - [14] Feng, W., Wang, P., Ding, X., Xu, L., Li, X.Q.: Generating and stabilizing the Greenberger-Horne-Zeilinger state in circuit QED: joint measurement, Zeno effect, and feedback. *Phys. Rev. A* **83**, 042313 (2011)
 - [15] Zhu, S.L., Wang, Z.D., Zanardi, P.: Geometric quantum computation and multiqubit entanglement with superconducting qubits inside a cavity. *Phys. Rev. Lett.* **94**, 100502 (2005)
 - [16] Bishop, L.S., et al.: Proposal for generating and detecting multi-qubit GHZ states in circuit QED. *New J. Phys.* **11**, 073040 (2009)
 - [17] Yang, C.P.: Preparation of n-qubit Greenberger-Horne-Zeilinger entangled states in cavity QED: an approach with tolerance to nonidentical qubit-cavity coupling constants. *Phys. Rev. A* **83**, 062302 (2011)
 - [18] Aldana, S., Wang, Y.D., Bruder, C.: Greenberger-Horne-Zeilinger generation protocol for N superconducting transmon qubits capacitively coupled to a quantum bus. *Phys. Rev. B* **84**, 134519 (2011)
 - [19] Imamoglu, A.: Cavity QED based on collective magnetic dipole coupling: spin ensembles as hybrid two-level systems. *Phys. Rev. Lett.* **102**, 083602 (2009)
 - [20] Wesenberg, J.H., Ardavan, A., Briggs, G.A., Morton, J.J.L., Schoellkopf, R.J., Schuster, D.I., Mømer K.: Quantum computing with an electron spin ensemble. *Phys. Rev. Lett.* **103**, 070502 (2009)
 - [21] Xiang, Z.L., Ashhab, S., You, J.Q., Nori, F.: Hybrid quantum circuits: superconducting circuits interacting with other quantum systems. *Rev. Mod. Phys.* **85**, 623 (2013)
 - [22] Xiang, Z.L., Lü, X.Y., Li, T.F., You, J.Q., Nori, F.: Hybrid quantum circuit consisting of a superconducting flux qubit coupled to a spin ensemble and a transmission-line resonator. *Phys. Rev. B* **87**, 144516 (2013)
 - [23] Lü, X.Y., Xiang, Z.L., Cui, W., You, J.Q., Nori, F.: Quantum memory using a hybrid circuit with flux qubits and nitrogen-vacancy centers. *Phys. Rev. A* **88**, 012329 (2013)
 - [24] Qiu, Y.Y., Xiong, W., Tian, L., You, J.Q.: Coupling spin ensembles via superconducting flux qubits. *Phys. Rev. A* **89**, 042321 (2014)

- [25] Song, W. L., Yin, Z. Q., Yang, W. L., Zhu, X., Zhou, F., Feng, M.: One-step generation of multipartite entanglement among nitrogen-vacancy center ensembles. *Sci. Rep.* **5**, 7755 (2015)
- [26] Tao, M. J., Hua, M., Ai, Q., Deng, F. G.: Quantum-information processing on nitrogen-vacancy ensembles with the local resonance assisted by circuit QED. *Phys. Rev. A* **91**, 062325 (2015)
- [27] Bar-Gill, N., Pham, L.M., Jarmola, A., Budker, D., Walsworth, R.L.: Solid-state electronic spin coherence time approaching one second. *Nat. Commun.* **4**, 1743 (2013)
- [28] Clarke, J., Wilhelm, F.K.: Superconducting quantum bits. *Nature* **453**, 1031 (2008)
- [29] You, J.Q., Nori, F.: Atomic physics and quantum optics using superconducting circuits. *Nature* **474**, 589 (2011)
- [30] Buluta, I., Ashhab, S., Nori, F.: Natural and artificial atoms for quantum computation. *Rep. Prog. Phys.* **74**, 104401 (2011)
- [31] Duan, L.M., Guo, G.C.: Reducing decoherence in quantum computer memory with all quantum bits coupling to the same environment. *Phys. Rev. A* **57**, 737 (1998)
- [32] Zhou, X., Wulf, M., Zhou, Z., Guo, G., Feldman, M.J.: Dispersive manipulation of paired superconducting qubits. *Phys. Rev. A* **69**, 030301(R) (2004)
- [33] Aolita, L., Davidovich, L., Kim, K., Häffner H.: Universal quantum computation in decoherence-free subspaces with hot trapped ions. *Phys. Rev. A* **75**, 052337 (2007)
- [34] Feng, Z.B., Zhang X.D.: Quantum computing in decoherence-free subspaces with superconducting charge qubits. *Phys. Lett. A* **372**, 16 (2007)
- [35] Xue, Z.Y., Wang Z.D., Zhu S.L.: Physical implementation of topologically decoherence-protected superconducting qubits. *Phys. Rev. A* **77**, 024301 (2008)
- [36] Wu, C.F., Feng X.L., Yi X.X., Chen I.M., Oh, C.H.: Quantum gate operations in the decoherence-free subspace of superconducting quantum-interference devices, *Phys. Rev. A* **78**, 062321 (2008)
- [37] Wang, Y.M., Zhou, Y.L., Liang, L.M., Li, C.Z.: Quantum Gate Operations in Decoherence-Free Subspace with Superconducting Charge Qubits inside a Cavity. *Chin. Phys. Lett.* **26**, 100304 (2009)
- [38] Hu, S., Cui, W.X., Guo, Q., Wang, H.F., Zhu, A.D., Zhang, S.: Multi-qubit non-adiabatic holonomic controlled quantum gates in decoherence-free subspaces. *arXiv:1601.02438*
- [39] Neeley, M., et al.: Process tomography of quantum memory in a Josephson-phase qubit coupled to a two-level state. *Nat. Phys.* **4**, 523 (2008)
- [40] Su, Q.P., Yang, C.P., Zheng, S.B.: Fast and simple scheme for generating NOON states of photons in circuit QED. *Sci. Rep.* **4**, 3898 (2014)
- [41] Yu, Y., Han, S. private communication.
- [42] Leek, P.J., et al.: Using sideband transitions for two-qubit operations in superconducting circuits. *Phys. Rev. B* **79**, 180511(R) (2009)
- [43] Strand, J.D., et al.: First-order sideband transitions with flux-driven asymmetric transmon qubits. *Phys. Rev. B* **87**, 220505(R) (2013)
- [44] Yang, W.L., Hu, Y., Yin, Z.Q., Deng, Z.J., Feng, M.: Entanglement of nitrogen-vacancy-center ensembles using transmission line resonators and a superconducting phase qubit. *Phys. Rev. A* **83**, 022302 (2011)
- [45] Neumann, P., Kolesov, R., Jacques, V., Beck, J., Tisler, J., Batalov, A., Rogers, L., Manson, N.B., Balasubramanian, G., Jelezko, F., Wrachtrup, J.: Excited-state spectroscopy of single NV defects in diamond using optically detected magnetic resonance. *New J. Phys.* **11**, 013017 (2009)
- [46] Pradhan, P., Anantram, M.P., Wang, K.L.: Quantum computation by optically coupled steady atoms/quantum-dots inside a quantum electro-dynamic cavity. *arXiv:quant-ph/0002006*
- [47] Yang, C.P., Han, S.: n-qubit-controlled phase gate with superconducting quantum interference devices coupled to a resonator. *Phys. Rev. A* **72**, 032311 (2005)
- [48] James, D.F.V., Jerke, J.: Effective Hamiltonian theory and its applications in quantum information. *Can. J. Phys.* **85**, 625 (2007)
- [49] Zheng, S.B., Guo, G.C.: Efficient scheme for two-atom entanglement and quantum information processing in cavity QED. *Phys. Rev. Lett.* **85**, 2392 (2000)
- [50] Sørensen, A., Mølmer, K.: Quantum computation with ions in thermal motion. *Phys. Rev. Lett.* **82**, 1971 (1999)
- [51] Brune, M., Hagley, E., Dreyer, J., Maitre, X., Maali, A., Wunderlich, C., Raimond, J. M., Haroche, S.: Observing the Progressive Decoherence of the “Meter” in a Quantum Measurement. *Phys. Rev. Lett.* **77**, 4887 (1996)
- [52] Palacios-Laloy, A., Nguyen, F., Mallet, F., Bertet, P., Vion, D., Esteve, D.: Tunable Resonators for Quantum Circuits. *J. Low Temp. Phys.* **151**, 1034 (2008)
- [53] Sandberg, M., Wilson, C.M., Persson, F., Bauch, T., Johansson, G. Shumeiko, V., Duty, T., Delsing, P.: Tuning the field in a microwave resonator faster than the photon lifetime. *Appl. Phys. Lett.* **92**, 203501 (2008)
- [54] Wang, Z.L., Zhong, Y.P., He, L.J., Wang, H., Martinis, J. M., Cleland, A. N., Xie, Q. W.: Quantum state characterization of a fast tunable superconducting resonator. *Appl. Phys. Lett.* **102**, 163503 (2013)
- [55] Hillery, M., Buzek, V., Berthiaume, A.: Quantum secret sharing. *Phys. Rev. A* **59**, 1829 (1999)
- [56] Nielsen, M.A., Chuang, I.L.: *Quantum Computation and Quantum Information* (Cambridge University Press, Cambridge, England, 2001)
- [57] Giovannetti, V., Vitali, D., Tombesi, P., Ekert, A.: Scalable quantum computation with cavity QED systems. *Phys. Rev. A* **62**, 032306 (2000)
- [58] He, X.L., Yang, C.P., Li, S., Luo, J.Y., Han, S.: Quantum logical gates with four-level superconducting quantum interference devices coupled to a superconducting resonator. *Phys. Rev. A* **82**, 024301 (2010)

- [59] Baur, M., Filipp, S., Bianchetti, R., Fink, J.M., Göppl, M., Steffen, L., Leek, P.J., Blais, A., Wallraff, A.: Measurement of Autler-Townes and Mollow Transitions in a Strongly Driven Superconducting Qubit. *Phys. Rev. Lett.* **102**, 243602 (2009).
- [60] Niemczyk, T., et al.: Circuit quantum electrodynamics in the ultrastrong-coupling regime. *Nat. Phys.* **6**, 772 (2010)
- [61] DiCarlo, L., et al.: Preparation and measurement of three-qubit entanglement in a superconducting circuit. *Nature* **467**, 574 (2010)
- [62] Stern, M., Catelani, G., Kubo, Y., Grezes, C., Bienfait, A., Vion, D., Esteve, D., Bertet P.: Flux Qubits with Long Coherence Times for Hybrid Quantum Circuits. *Phys. Rev. Lett.* **113**, 123601 (2014)
- [63] Chang, J.B., et al.: Improved superconducting qubit coherence using titanium nitride. *Appl. Phys. Lett.* **103**, 012602 (2013)
- [64] Peterer M.J., Bader, S.J., Jin, X., Yan, F., Kamal, A., Gudmundsen, T.J., Leek, P.J., Orlando, T.P., Oliver, W.D., Gustavsson, S.: Coherence and Decay of Higher Energy Levels of a Superconducting Transmon Qubit. *Phys. Rev. Lett.* **114**, 010501 (2015)
- [65] Chen, W., Bennett, D.A., Patel, V., Lukens, J.E.: Substrate and process dependent losses in superconducting thin film resonators. *Supercond. Sci. Technol.* **21**, 075013 (2008)
- [66] Leek, P.J., Baur, M., Fink, J.M., Bianchetti, R., Steffen, L., Filipp, S., Wallraff, A.: Cavity quantum electrodynamics with separate photon storage and qubit readout modes. *Phys. Rev. Lett.* **104**, 100504 (2010)